

Far field emission profile of pure wurtzite InP nanowires

Gabriele Bulgarini¹, Dan Dalacu, Philip J. Poole, Jean Lapointe, Michael E. Reimer, and Val Zwiller

Citation: *Appl. Phys. Lett.* **105**, 191113 (2014); doi: 10.1063/1.4901437

View online: <http://dx.doi.org/10.1063/1.4901437>

View Table of Contents: <http://aip.scitation.org/toc/apl/105/19>

Published by the [American Institute of Physics](#)



**FIND THE NEEDLE IN THE
HIRING HAYSTACK**

POST JOBS AND REACH THOUSANDS OF
QUALIFIED SCIENTISTS EACH MONTH.

PHYSICS TODAY | JOBS
WWW.PHYSICSTODAY.ORG/JOBS

Far field emission profile of pure wurtzite InP nanowires

Gabriele Bulgarini,^{1,a)} Dan Dalacu,² Philip J. Poole,² Jean Lapointe,² Michael E. Reimer,¹ and Val Zwiller¹

¹Kavli Institute of Nanoscience, Delft University of Technology, Delft, The Netherlands

²National Research Council, Ottawa, Ontario, K1A 0R6, Canada

(Received 1 July 2014; accepted 30 October 2014; published online 12 November 2014)

We report on the far field emission profile of pure wurtzite InP nanowires in comparison to InP nanowires with predominantly zincblende crystal structure. The emission profile is measured on individual nanowires using Fourier microscopy. The most intense photoluminescence of wurtzite nanowires is collected at small angles with respect to the nanowire growth axis. In contrast, zincblende nanowires present a minimum of the collected light intensity in the direction of the nanowire growth. Results are explained by the orientation of electric dipoles responsible for the photoluminescence, which is different from wurtzite to zincblende. Wurtzite nanowires have dipoles oriented perpendicular to the nanowire growth direction, whereas zincblende nanowires have dipoles oriented along the nanowire axis. This interpretation is confirmed by both numerical simulations and polarization dependent photoluminescence spectroscopy. Knowledge of the dipole orientation in nanostructures is crucial for developing a wide range of photonic devices such as light-emitting diodes, photodetectors, and solar cells. © 2014 AIP Publishing LLC.

[<http://dx.doi.org/10.1063/1.4901437>]

Semiconductor nanowires have drawn increasing attention in recent years because of their possible applications in a large variety of fields that ranges from photovoltaic,^{1,2} photodetection,^{3,4} biological sensing,⁵ to quantum information.^{6,7} Key advantages of nanowires, compared to their bulk counterpart, are that more material combinations⁸ and crystalline structures are available using nanowire growth. For example, a wurtzite crystal structure is achieved in GaP⁹ and InP¹⁰ nanowires, which are not stable in bulk growth.

Recent discussion in the scientific community has centered around the optical polarization properties of wurtzite InP nanowires.^{11–13} Zincblende nanowires emit light polarized along the nanowire elongation axis that is the direction of the nanowire growth. On the contrary, light emitted from wurtzite nanowires is found to be polarized perpendicular to the nanowire elongation axis. This effect owes to the different order of the atoms in the crystal resulting in different optical selection rules. Seminal experiments suggesting an orientation of the optical dipoles perpendicular to the nanowire were reported by Mishra *et al.*¹¹ The dipole orientation was measured via polarization dependent photoluminescence spectroscopy. Subsequent work from other groups established these results.^{12,13} Here, we use Fourier microscopy to measure the dipole orientation in nanowires. We measure the far field emission profile of individual wurtzite and zincblende nanowires. Experimental results are compared with finite-difference time-domain (FDTD) simulations. Furthermore, our Fourier microscopy results are supported by polarization dependent photoluminescence on individual free-standing nanowires.

Figure 1 shows the result of numerical simulations for the nanowire far field emission profile. The model accounts for an InP nanowire with hexagonal cross section, as

displayed in Figs. 1(a) and 1(c), with a side of 110 nm. This structure is equivalent to a cylinder with diameter of 200 nm.¹⁴ We simulate the nanowire emission using an electric dipole located on the nanowire axis at half of the nanowire length, similarly to Grzela *et al.* in Ref. 15. Simulating a single point-like dipole produces similar results to a spatial average of the dipole locations along the nanowire.¹⁵ The spectral range for the dipolar emission is 850 ± 20 nm in order to account for both the zincblende and wurtzite crystal structure in the simulation. Fig. 1(a) depicts a nanowire with electric dipole oriented along the nanowire axis. The dipole orientation is displayed by the double-sided arrow. The angular distribution of the power emitted by a radiating dipole positioned in vacuum follows a $\sin^2\phi$ dependence,¹⁶ where $\phi = 0$ is the direction along the dipole orientation. Hence, light is expected to be emitted in a direction perpendicular to the dipole orientation and none of the light is expected to be collected in the direction parallel to the dipole. However, the presence of a dielectric medium surrounding the radiating dipole or of a dielectric interface modifies the emission profile.¹⁷ Numerical solutions of Maxwell's equations for a dipole oriented parallel to the nanowire axis yield the far field profile shown in Fig. 1(b). The intensity of the light electric field is color-coded and is plotted as a function of the light transverse \mathbf{k} -vector. The transverse \mathbf{k} -vector is perpendicular to the photon propagation direction, z , as displayed in Figs. 1(a) and 1(c). The simulation results are displayed in Figs. 1(b) and 1(d) as a function of the two \mathbf{k} -vector in-plane components: k_x and k_y . The emission angle, ϕ , is related to the \mathbf{k} -vector by: $\mathbf{k} = \arcsin \phi$. We observe a minimum of the electric field intensity for $\mathbf{k} = 0$ as a consequence of the dipole orientation. The angular distribution of the electric field has a doughnut-shape. In Fig. 1(c), a nanowire with electric dipoles oriented perpendicular to the nanowire axis is displayed. The calculated far field emission profile, shown in

^{a)}Electronic mail: g.bulgarini@tudelft.nl

Fig. 1(d), presents a pronounced maximum at $\mathbf{k} = 0$ in stark contrast with the profile calculated for a parallel dipole in Fig. 1(b).

We now discuss experimental results of Fourier microscopy on individual nanowires. The sample is kept at cryogenic temperature (~ 5 K) and is optically excited by a continuous-wave HeNe laser at 633 nm. Photoluminescence from the nanowire is collected by a high numerical aperture objective, NA of 0.8, which according to the simulations should ensure near-unity collection of the nanowire emission propagating upwards. We display the collection NA with a white dashed circle in the simulations of Figs. 1(b) and 1(d). The light intensity distribution on the back focal plane of the objective represents the photoluminescence intensity as a function of the emission angle. In other words, the back focal plane of the objective contains the information of the Fourier plane of the emitter. For imaging the light intensity in k -space, we position a lens at equal distance between the objective and a charge-coupled device (CCD) camera. A schematic of the experimental setup can be found in Ref. 18. The light intensity distribution is reproduced as a 1:1 image on the CCD camera for a distance $2f$ between lens and objective and an additional distance $2f$ from the lens to the CCD camera. In the experimental setup, the laser reflection is blocked by a thin-film dielectric filter positioned along the collection optical path. This filter does not affect the \mathbf{k} -vector information of the nanowire luminescence.

Photoluminescence spectroscopy performed at cryogenic temperature (~ 5 K) on an individual pure wurtzite nanowire is shown in Fig. 2(a). We observe the band-edge luminescence (WZ) at 832 nm, which dominates the spectrum. At

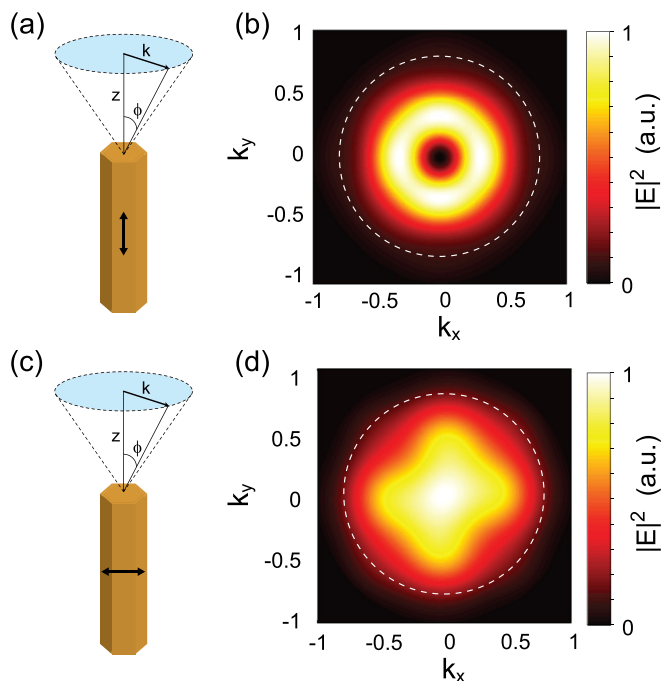


FIG. 1. Numerical simulations of the nanowire emission profile. (a) A nanowire with an electric dipole (arrow) aligned along the nanowire axis. The nanowire has a hexagonal cross section (side = 110 nm, equivalent to a cylinder with diameter of 200 nm) and the emission wavelength is 850 ± 20 nm. (b) Calculated far field emission profile from (a). A white dashed circle is indicating the collection numerical aperture of 0.8. (c) A nanowire with dipole perpendicular to the growth axis. (d) Calculated far field emission profile from (c). The electric field intensity profile is maximum for $\mathbf{k} = 0$.

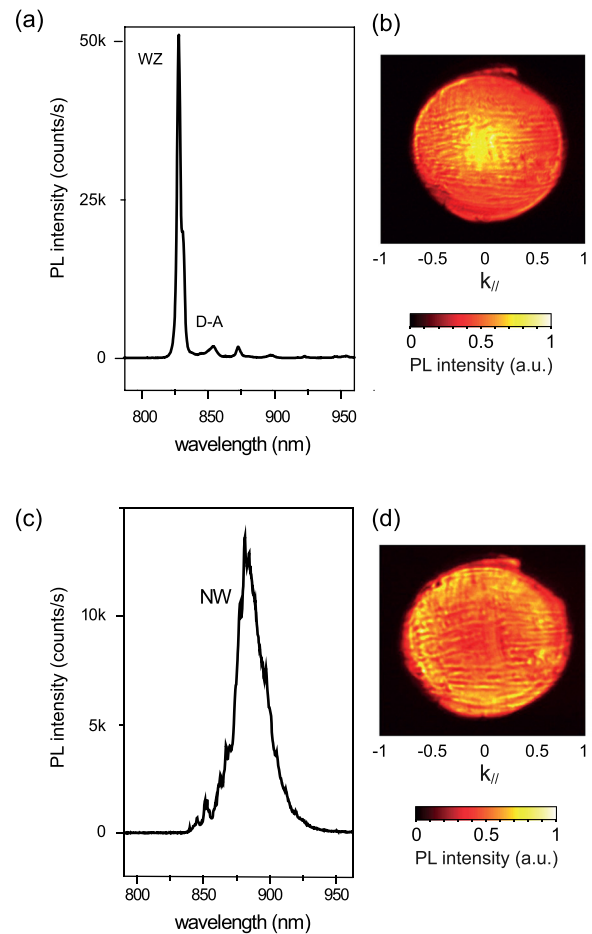


FIG. 2. Fourier microscopy of individual nanowires. (a) Photoluminescence spectrum of an individual InP nanowire with pure wurtzite crystal structure. (b) Far field emission profile of a wurtzite nanowire. The emission intensity is maximum for $\mathbf{k} = 0$. (c) Photoluminescence spectrum of an individual nanowire with predominantly zincblende crystal structure. (d) Far field emission profile of a zincblende nanowire.

longer wavelength, we measure luminescence collected from the donor-acceptor transitions (D-A), at 860 nm. To achieve pure crystal phase, nanowires are grown by chemical beam epitaxy with a two-step growth process on an InP substrate covered by a SiO_2 mask composed of holes defined via electron-beam lithography. First, the nanowire is grown with a small diameter of ~ 20 nm. For this nanowire dimension, the nanowire crystal phase is wurtzite and contains a very low stacking fault density of less than one per micron.¹⁰ Subsequently, growth from the substrate is promoted and InP forms a shell around the nanowire core. The shell maintains the pure wurtzite crystalline order of the core.

We now measure the photoluminescence intensity in Fourier space for the wurtzite band-edge transition. The Fourier image of the emission from an individual nanowire is shown in Fig. 2(b). The emission intensity is maximum in the direction parallel to the nanowire axis ($\mathbf{k} = 0$). This experimental result is consistent with the orientation of electric dipoles perpendicular to the nanowire axis as shown in the calculations from Fig. 1(d).

Next, we measure the far field emission profile from individual nanowires of similar dimensions, but consisting mainly of zincblende crystal structure. A photoluminescence spectrum is shown in Fig. 2(c). We observe a broad nanowire

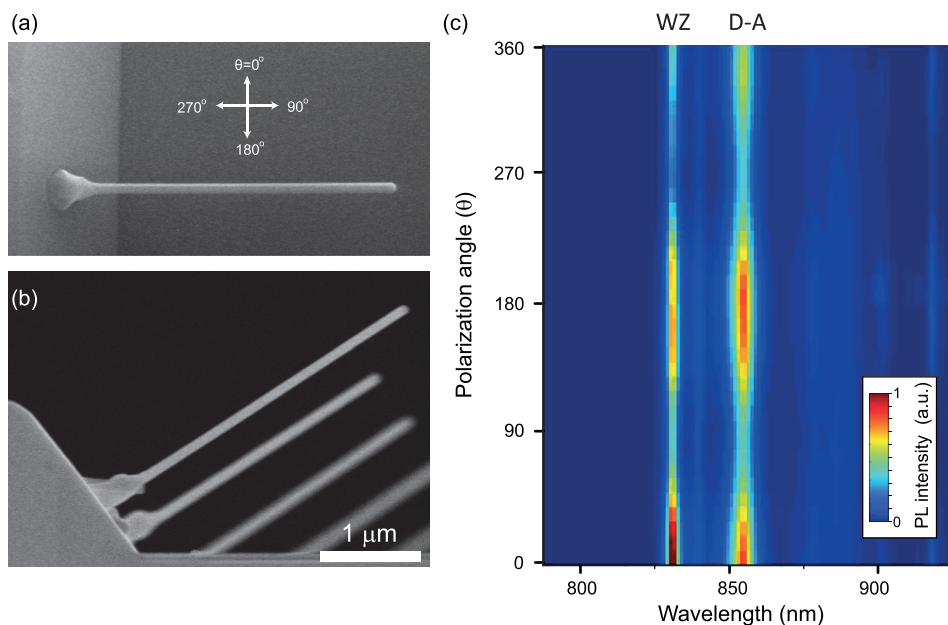


FIG. 3. Polarization dependent photoluminescence of a wurtzite nanowire. (a) and (b) Scanning electron microscopy (SEM) image of individual nanowires grown on a ridge. The employed polarization coordinates of the collection optics are displayed by the arrows with respect to the nanowire orientation in (a). (b) Nanowires are grown at a 35 degree angle with respect to the substrate. (c) Polarization dependent photoluminescence of the wurtzite nanowire band-edge emission collected from the top of the ridges. The most intense photoluminescence is collected for polarization perpendicular to the nanowire axis. The photoluminescence intensity is color-coded.

emission centered around ~ 870 nm. The broader nanowire emission as compared to the wurtzite emission peak shown in Fig. 2(a) is ascribed to stacking faults along the nanowire,¹⁹ which have a yet unknown dipole orientation. The far field emission profile of this nanowire emission is presented in Fig. 2(d). We observe a doughnut shape that is consistent with dipoles oriented along the nanowire axis and with previous observations reported in the literature.¹⁵

Fourier imaging in combination with FDTD simulations of the far-field emission profile confirms that wurtzite nanowire photoluminescence results from dipoles aligned perpendicular to the nanowire axis. As a result of the dipole orientation, the emission is collected from the top of the nanowire, along the growth direction, at small emission angles. In order to confirm this interpretation of the results, we perform polarization-resolved photoluminescence spectroscopy. In these measurements, we utilize individual wurtzite nanowires grown on ridges, as shown in Figure 3(b). For the creation of ridges, a rectangular mask is utilized to etch a (001) InP substrate. Subsequent growth on such patterned substrate develops a structure with trapezoidal cross-section due to material migration towards the (001) apex. Nanowire growth occurs on the (111)B facets which are exposed on the sidewalls of the trapezoid, as explained in a more detailed description in Ref. 20. Prior to the nanowire growth, gold droplets are patterned on the ridge sidewalls in order to provide site-selective catalyzed growth of isolated single nanowires. First, circular openings defined by electron beam lithography are etched in SiO₂ covered ridges. Next, a 10 nm gold layer is deposited uniquely inside the etched openings providing the catalyst material to the vapour-liquid-solid nanowire growth. The use of nanowires grown on ridges provides a very clean measurement for polarization-resolved photoluminescence spectroscopy, because it avoids the transfer of nanowires to another substrate where the dielectric material may alter the measurement.¹⁷ The results of polarization-resolved photoluminescence spectroscopy are shown in Fig. 3(c). In the measurements, photoluminescence is collected from the top

of the ridges. The nanowire photoluminescence intensity is maximum for light polarized perpendicular to the nanowire axis ($\theta = 0$) and minimum for polarization along the nanowire. This polarization orientation is ascribed to radiating electric dipoles aligned perpendicular to the nanowire axis for the wurtzite crystal phase, as previously suggested for explaining the far field emission patterns. We observe a strong degree of polarization of on average $\sim 60\%$, which is slightly higher than the 49% reported from Mishra *et al.*,¹¹ using a single wurtzite InP nanowires lying on a silicon substrate. The interaction of the electric dipoles in the nanowire with the dielectric environment alters the optical selection rules yielding a lower degree of polarization.

We have reported Fourier microscopy measurements on pure InP wurtzite nanowires as compared to nanowires with a predominantly zincblende crystal structure. The measurements indicate that electric dipoles responsible for the band-edge photoluminescence in wurtzite nanowires are aligned perpendicular to the nanowire axis. In consequence, the photoluminescence is collected at small angles in the far field. In contrast, an opposite dipole orientation is observed for zincblende nanowires. Fourier images of zincblende emission exhibit a doughnut-like emission profile which is in agreement with dipoles oriented parallel to the nanowire axis. The interpretation of the Fourier microscopy results is further confirmed by polarization-resolved photoluminescence spectroscopy on individual nanowires and FDTD simulations.

Our findings are extremely important for the development of future nanowire devices where control of the emission profile is a prerogative, for instance, light-emitting diodes²¹ and lasers.²² Moreover, the fundamental difference in electric dipole orientations between zincblende and wurtzite nanowires is important in applications where engineering the light absorption is crucial such as photovoltaic and photodetection. We remark that the investigation of both the wurtzite and zincblende crystal structure is only possible with nanowires where, by tuning the growth parameters, different crystal structures are obtained with a versatility which is not possible in bulk growth.

The authors acknowledge E. P. A. M. Bakkers for the growth of zincblende nanowires. This work was supported by the Netherlands Organization for Scientific Research (NWO), Dutch Organization for Fundamental Research on Matter (FOM), and European Research Council.

- ¹M. D. Kelzenberg, S. W. Boettcher, J. A. Petykiewicz, D. B. Turner-Evans, M. C. Putnam, E. L. Warren, J. M. Spurgeon, R. M. Briggs, N. S. Lewis, and H. A. Atwater, *Nature Mater.* **9**, 368 (2010).
- ²J. Wallentin, N. Anttu, D. Asoli, M. Huffman, I. Åberg, M. H. Magnusson, G. Siefer, P. Fuss-Kailuweit, F. Dimroth, B. Witzigmann *et al.*, "InP nanowire array solar cells achieving 13.8% efficiency by exceeding the ray optics limit," *Science* **339**, 1057–1060 (2013).
- ³O. Hayden, R. Agarwal, and C. M. Lieber, "Nanoscale avalanche photodiodes for highly sensitive and spatially resolved photon detection," *Nature Mater.* **5**, 352–356 (2006).
- ⁴G. Bulgarini, M. E. Reimer, M. Hocevar, E. P. A. M. Bakkers, L. P. Kouwenhoven, and V. Zwiller, "Avalanche amplification of a single exciton in a semiconductor nanowire," *Nat. Photon.* **6**, 455–458 (2012).
- ⁵J. T. Robinson, M. Jorgolli, A. K. Shalek, M.-H. Yoon, R. S. Gertner, and H. Park, "Vertical nanowire electrode arrays as a scalable platform for intracellular interfacing to neuronal circuits," *Nat. Nanotechnol.* **7**, 180–184 (2012).
- ⁶J. Claudon, J. Bleuse, N. S. Malik, M. Bazin, P. Jaffrennou, N. Gregersen, C. Sauvan, P. Lalanne, and J.-M. Gerard, "A highly efficient single-photon source based on a quantum dot in a photonic nanowire," *Nat. Photon.* **4**, 174–177 (2010).
- ⁷M. E. Reimer, G. Bulgarini, N. Akopian, M. Hocevar, M. Bouwes Bavinck, M. A. Verheijen, Erik P. A. M. Bakkers, L. P. Kouwenhoven, and V. Zwiller, "Bright single-photon sources in bottom-up tailored nanowires," *Nat. Commun.* **3**, 737 (2012).
- ⁸S. R. Plissard, D. R. Slapak, M. A. Verheijen, M. Hocevar, G. W. G. Immink, I. van Weperen, S. Nadj-Perge, S. M. Frolov, L. P. Kouwenhoven, and E. P. A. M. Bakkers, "From InSb nanowires to nanocubes: Looking for the sweet spot," *Nano Lett.* **12**, 1794–1798 (2012).
- ⁹S. Assali, I. Zardo, S. Plissard, D. Krieger, M. A. Verheijen, G. Bauer, A. Meijerink, A. Belabbes, F. Bechstedt, J. E. M. Haverkort, and E. P. A. M. Bakkers, "Direct band gap wurtzite gallium phosphide nanowires," *Nano Lett.* **13**, 1559–1563 (2013).
- ¹⁰D. Dalacu, K. Mnaymeh, J. Lapointe, X. Wu, P. J. Poole, G. Bulgarini, V. Zwiller, and M. E. Reimer, "Ultraclean emission from InAsP quantum dots in defect-free wurtzite InP nanowires," *Nano Lett.* **12**, 5919–5923 (2012).
- ¹¹A. Mishra, L. V. Titova, T. B. Hoang, H. E. Jackson, L. M. Smith, J. M. Yarrison-Rice, Y. Kim, H. J. Joyce, Q. Gao, H. H. Tan, and C. Jagadish, "Polarization and temperature dependence of photoluminescence from zincblende and wurtzite InP nanowires," *Appl. Phys. Lett.* **91**, 263104 (2007).
- ¹²D. Spirkoska, Al. L. Efros, W. R. L. Lambrecht, T. Cheiwchanchamnangij, A. Fontcuberta i Morral, and G. Abstreiter, "Valence band structure of polytypic zinc-blende/wurtzite GaAs nanowires probed by polarization-dependent photoluminescence," *Phys. Rev. B* **85**, 045309 (2012).
- ¹³Y. Masumoto, Y. Hirata, P. Mohan, J. Motohisa, and T. Fukui, "Polarized photoluminescence from single wurtzite InP/InAs/InP core-multishell nanowires," *Appl. Phys. Lett.* **98**, 211902 (2011).
- ¹⁴A.-L. Henneghien, B. Gayral, Y. Désières, and J.-M. Gérard, "Simulation of waveguiding and emitting properties of semiconductor nanowires with hexagonal or circular sections," *J. Opt. Soc. Am. B* **26**, 2396–2403 (2009).
- ¹⁵G. Grzela, R. Paniagua-Dominguez, T. Barten, Y. Fontana, J. Sanchez-Gil, and J. Gomez Rivas, "Nanowire antenna emission," *Nano Lett.* **12**, 5481–5486 (2012).
- ¹⁶W. Lukosz and R. E. Kunz, "Light emission by magnetic and electric dipoles close to a plane interface. I. Total radiated power," *J. Opt. Soc. Am.* **67**, 1607–1615 (1977).
- ¹⁷G. Bulgarini, M. E. Reimer, and V. Zwiller, "Optical polarization properties of a nanowire quantum dot probed along perpendicular orientations," *Appl. Phys. Lett.* **101**, 111112 (2012).
- ¹⁸G. Bulgarini, M. E. Reimer, M. Bouwes Bavinck, K. D. Jöns, D. Dalacu, P. J. Poole, E. P. A. M. Bakkers, and V. Zwiller, "Nanowire waveguides launching single photons in a Gaussian mode for ideal fiber coupling," *Nano Lett.* **14**, 4102–4106 (2014).
- ¹⁹N. Akopian, G. Patriarche, L. Liu, J.-C. Harmand, and V. Zwiller, "Crystal phase quantum dots," *Nano Lett.* **10**, 1198–1201 (2010).
- ²⁰D. Dalacu, A. Kam, D. G. Austing, and P. J. Poole, "Droplet dynamics in controlled InAs nanowire interconnections," *Nano Lett.* **13**, 2676–2681 (2013).
- ²¹K. Tomioka, J. Motohisa, S. Hara, K. Hiruma, and T. Fukui, "GaAs/AlGaAs core multishell nanowire-based light-emitting diodes on Si," *Nano Lett.* **10**, 1639–1644 (2010).
- ²²M. A. Zimmler, J. Bao, F. Capasso, S. Mueller, and C. Ronning, "Laser action in nanowires: Observation of the transition from amplified spontaneous emission to laser oscillation," *Appl. Phys. Lett.* **93**, 051101 (2008).